Buckling Pneumatic Linear Actuators Inspired by Muscle

*Dian Yang, Mohit S. Verma, Ju-Hee So, Bobak Mosadegh, Christoph Keplinger, Benjamin Lee, Fatemeh Khashai, Elton Lossner, Zhigang Suo, and George M. Whitesides**

Soft actuators possess the ability to contact delicate, soft, and irregularly shaped objects (for example, fruit, animals, or clothing), because they distribute force across the surface of the objects, and because they are fabricated of compliant rather than unyielding materials.[1–8] They also offer an attractive approach to simplifying control,[5–8] since they make it possible—in some circumstances—to substitute the properties of soft materials and structures for some of the control loops, sensors, and actuators of hard machines (machines fabricated in metals, ceramics, and structural polymers).[9,10] The simplification of control is important in the field of robotics as a potential strategy for designing robots that work in unstructured environments.[11]

Mechanical instabilities—here, the buckling of beams—are usually considered mechanisms of failure in hard structures.[12–14] An emerging opportunity in the engineering of soft machines is to harness these instabilities to achieve new functionalities.[15–17] For example, buckling has proven useful in the design of stretchable soft electronics,[18,19] tunable materials,[20–23] and fluidic actuators.[24] We have previously demonstrated that reversible buckling of elastomeric beams can be used to make a torsional soft actuator.[25]

This paper demonstrates that reversible buckling in assemblies of elastomeric beams can generate motions similar to those of skeletal muscles. Elastomeric pneumatic actuators based on buckling have, so far, demonstrated only rotation.[25] The actuators we describe here—vacuum-actuated muscle-inspired pneumatic structures (VAMPs)—differ from these previous elastomeric pneumatic actuators because they generate a linear motion, which resembles the motion of linear actuators in rigid robots (e.g., pistons and motor-actuated cables) and animals (e.g., muscle). VAMPs use buckling of elastomeric beams to generate muscle-like motions when negative pressure (vacuum) is applied to them; the external (ambient) pressure causes their cooperative, reversible collapse (that is, buckling).[26] Like biological muscles, VAMPs are soft, and thus able to absorb shock, and to interact nondestructively with their environment and collaboratively with humans. VAMPs also have a cellular structure, which has the potential to allow repair after damage. In contrast to previous soft actuators, which often move by expanding under pressure, VAMPs are similar to muscle in that they do not expand in cross-sectional area during actuation (although they contract in total volume); these geometrical features allow them to operate in space-constrained environments. The fact that VAMPs are made of elastomers allows them to store and release elastic energy. VAMPs can generate linear motions with strains up to 45%, and can sustain loading stresses up to 65 kPa (the theoretical maximum being 100 kPa under atmospheric pressure, with even higher values possible in hyperbaric environments); both strain and stress are similar to those of human muscle (typical strains of ≈20%, with maximum values up to ≈40%; maximum sustained stress of ≈100 kPa, and maximum impulsive stress of ≈350 kPa).[27] We also demonstrate that VAMPs made of Elastosil demonstrate a reasonable thermodynamic efficiency (≈27% efficiency at 20% strain without optimization); this value is within a factor of two of that of human muscle (≈40% efficiency).[27]

The history of muscle-like actuators is long. Among many such actuators, the McKibben actuator, developed in the 1950s, and its relatives (other braided muscle, knitted muscle, pleated muscle, etc.[28]) were the first truly successful examples.[29] A typical McKibben actuator comprises a rubber balloon, constrained in volume by an inelastic mesh. On pressurization, the anisotropic inflation of this balloon results in useful motion. The properties of the mesh (i.e., the density of the weave, and the strength of the fibers) dictate the strain (typically 25%) and stress (typically 800–1300 kPa) the actuator can produce for a given applied pneumatic pressure (typically ≈500 kPa).[30] McKibben actuators have many practical applications, but have three characteristics that can limit their utility:[28] (i) Their inherent dry friction, and the nonelastic deformation of the mesh balloon, causes hysteresis; this hysteresis renders precise positional control difficult. (ii) They often cannot be actuated if the applied pressure is below a certain "threshold pressure"; this threshold may prevent the generation of low force. (iii) The application of a pressure that is too high (typically ≈500 kPa) can make the balloon bulge through the mesh or at a point of damage, and perhaps burst. Other thoughtfully designed types of actuators (driven by electricity, temperature, and other means) have also been developed to mimic properties of the muscle.[27,31–33]

Dr. D. Yang, Dr. M. S. Verma, Dr. J.-H. So, Prof. B. Mosadegh, Prof. C. Keplinger, B. Lee, F. Khashai, E. Lossner, Prof. G. M. Whitesides
Department of Chemistry and Chemical Biology
Harvard University
12 Oxford Street, Cambridge, MA 02138, USA
E-mail: gwhitesides@gmwgroup.harvard.edu
Dr. D. Yang, Prof. Z. Suo
School of Engineering and Applied Sciences
Harvard University
29 Oxford Street, Cambridge, MA 02138, USA
Prof. B. Mosadegh, Prof. G. M. Whitesides
Wyss Institute for Biologically Inspired Engineering
Harvard University
60 Oxford Street, Cambridge, MA 02138, USA
Prof. Z. Suo, Prof. G. M. Whitesides
Kavli Institute for Bionano Science & Technology
Harvard University
29 Oxford Street, Cambridge, MA 02138, USA

DOI: 10.1002/admt.201600055

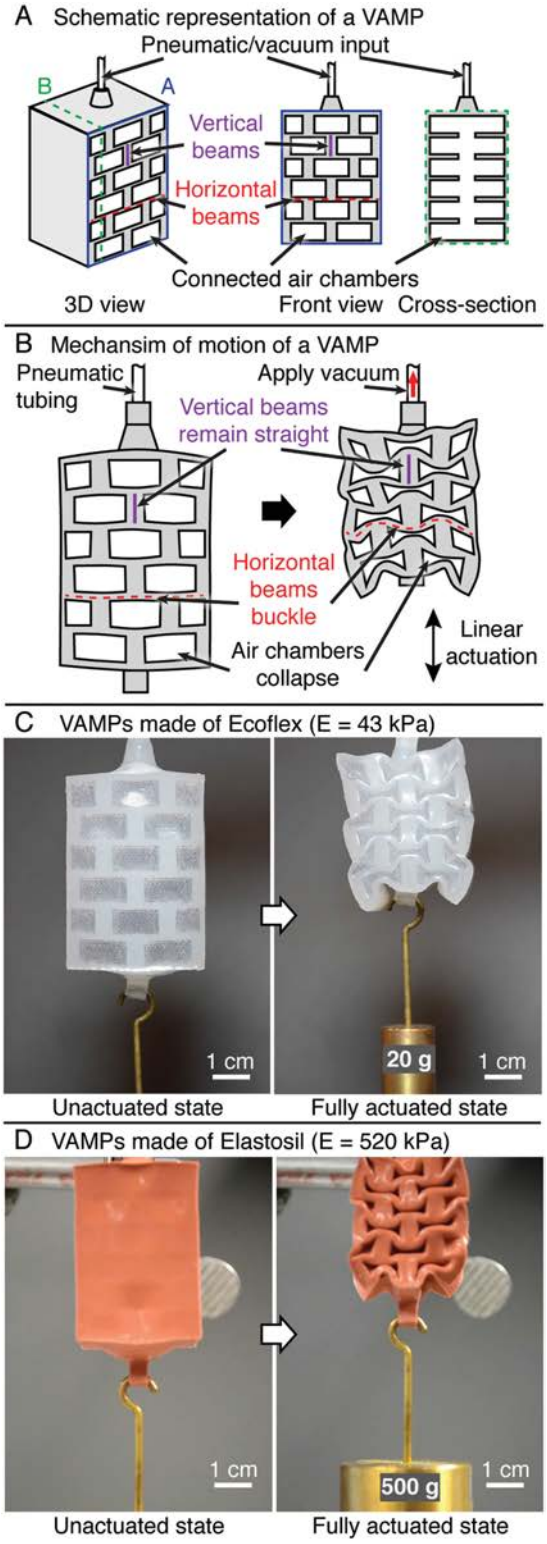

Figure 1. Schematic description of VAMPs. A) A VAMP consists of an elastomeric structure of vertical beams, thinner horizontal beams, and connected air chambers. The device is actuated using a single external port and a source of vacuum. B) The vacuum allows ambient pressure to compress the structure, and thus to cause the thinner horizontal beams to buckle into serpentine shapes, which in turn causes the structure to compress anisotropically. C) Images of a VAMP made of Ecoflex ($E = 43$ kPa) lifting a small weight (20 g) when actuated by applying a vacuum. The inside of the chamber membranes of this VAMP is colored with a black marker, such that the boundaries of the chambers are more visible in the actuated state. D) A VAMP of the same geometry as in (C), but made of Elastosil ($E = 520$ kPa) lifts a much higher weight (500 g). As Elastosil is not transparent, the chambers of this VAMP are not visible in the unactuated state, but more visible in the actuated state as the membrane bends inward. Scale bars are 1 cm. See Movies S1 and S2 (Supporting Information) for the videos. Figure S2 and Movie S3 (Supporting Information) demonstrate VAMPs with even higher strength.

Actuators that operate based on negative pressure (vacuum) have been less explored than those using positive pressure, although they have two advantages: (i) they cannot burst (nor can they "implode," as the actuation stops when the pneumatic chambers collapse to their minimum volume); (ii) their volume decreases on application of vacuum (which allows them to function better in cluttered or space-constrained environments than actuators using positive pressure). Jaeger and co-workers described an example of this type of actuator, in which application of vacuum to an elastomeric bag filled with a granular solid caused jamming; this jamming increased the stiffness of the bag and its contents, and allowed gripping.[5]

Our research was stimulated by work of Boyce and co-workers, who demonstrated regular structural deformations in periodic elastomeric cellular solids—slabs of elastomer containing arrays of circular holes perpendicular to the slab—upon application of mechanical force in the plane of the slab.[34,35] Our structures are based on a different elastomeric structure that can be considered to comprise a number of interacting elastic beams and interconnected, deformable cavities sealed within a thin elastomeric membrane (**Figure 1**). Application of vacuum to the cavities causes the ambient atmospheric pressure to compress the device isotropically; this compression results in reversible, cooperative buckling of the beams, and in an anisotropic change in the shape of the structure. This design converts pressure–volume work (done by applying negative pressure) into mechanical work (here, for example, lifting a weight).

The pattern of beams (or, equivalently, the pattern of voids in the elastomeric slab) we use is partially inspired by the auxetic structure discovered by Travesset and co-workers—a network of stiff levers that resembles the pattern of mortar in a brick wall.[36] In one of our designs for VAMPs, the pattern consists of long, thin (1.5 mm) horizontal beams, bridged by thick (4 mm) vertical beams (Figure 1A and Figure S1 (Supporting Information) summarize details of fabrication; the Supporting Information also discusses how the behavior of the structure changes as the size of the features is increased and provides a modeling approach). When vacuum is applied to the structure, the horizontal beams buckle reversibly into serpentine shapes, and this buckling results in a large change in the vertical length of the structure (≈40%), but a much smaller change (≈5%) in its horizontal width (Figure 1B–D and Movies S1 and S2 (Supporting Information)).

We characterized two mechanical relationships for VAMPs (with dimension 34 mm × 28 mm × 46.5 mm) under quasi-static conditions: those between (i) applied differential pressure and change in length with no load; and (ii) Young's modulus of

the elastomer and the maximum load the structure can lift (that is, the force it can apply). We first define two variables: (i) the difference in pressure, ΔP, between the external ambient pressure P_{ext} (typically ≈1 atm ≈ 100 kPa) and the pressure inside the chambers P_{int} when under reduced pressure (Equation (1)); and (ii) the loading stress σ (in kPa) resulting from a weight applied to the VAMP (Equation (2)). Here, T is the force in the direction of actuation, and A is the cross-sectional area of the undeformed actuator

$$\Delta P = P_{ext} - P_{int} \tag{1}$$

$$\sigma = \frac{T}{A}. \tag{2}$$

The actuation strain $s(\Delta P,\sigma)$ (i.e., the strain induced by actuation, rather than by external loading) is a function of these two variables (Equation (3)), where $L(\Delta P,\sigma)$ is the length of the VAMP under loading stress σ on application of a differential pressure ΔP

$$s(\Delta P,\sigma) = \frac{L(\Delta P,\sigma) - L(0,\sigma)}{L(0,0)}. \tag{3}$$

Figure 2A,B shows the actuation strain of VAMPs under zero loading stress $s(\Delta P,0)$. As the differential pressure ΔP increases, the VAMPs contract along their long axis, initially approximately linearly. Above a certain value (ΔP_{crit}) of ΔP (which depends on the properties of the elastomer), the VAMPs collapse almost completely. For Ecoflex 00-30 (Young's modulus E = 43 kPa), ΔP_{crit} is about 1 kPa; for Elastosil M4601 (E = 520 kPa), ΔP_{crit} is about 10 kPa. This critical differential pressure is proportional to the Young's modulus of the material (see the Supporting Information for a theoretical validation). Hence, VAMPs made of a material with critical Young's modulus $E \approx 5$ MPa will have a ΔP_{crit} of ≈100 kPa (1 atm), which is the largest pressure differential a vacuum system can provide at atmospheric pressure. This scaling rule describes the stiffness of the material of which VAMPs can be fabricated. In addition, the approximately linear relationship between the strain $s(\Delta P,0)$ and applied pressure ΔP (for $\Delta P < \Delta P_{crit}$) shown in Figure 2A,B implies that VAMPs can stably (<1% change in height; details are in the Supporting Information) maintain any particular achievable strain $s(\Delta P,0)$ given an applied pressure ΔP; this capability suggests that they should be easy to control.

Figure 2C,D shows the actuation strain $s(\Delta P,\sigma)$ of VAMPs made of two different elastomers as a function of loading stress σ, while applying a negative pressure greater than ΔP_{crit}. At a

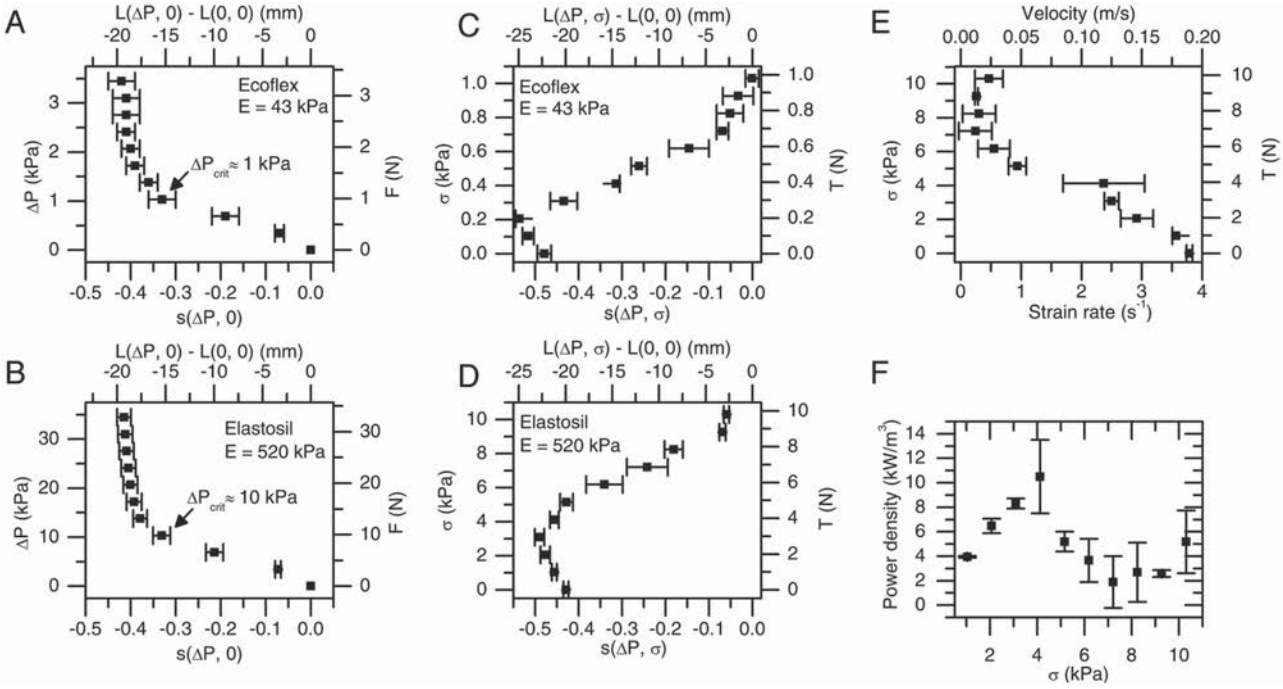

Figure 2. Static and dynamic characteristics of VAMPs. A,B) Applied differential pressure ΔP versus actuation strain $s(\Delta P,0)$ curves of seven different VAMPs made of Ecoflex (E = 43 kPa) and Elastosil (E = 520 kPa) at no load. The critical differential pressure (ΔP_{crit}) at which VAMPs compress almost completely is proportional to the Young's modulus of the material. C,D) Loading stress σ versus actuation strain $s(\Delta P,\sigma)$ curves of seven different VAMPs made of Ecoflex (E = 43 kPa) and Elastosil (E = 520 kPa), when a differential pressure of ΔP = 90 kPa is applied (i.e., force–length relationship under active loading). A VAMP exerts greater force when fabricated in a stiffer elastomer—an approximately tenfold increase in the modulus of material results in an approximately tenfold increase in loading stress. (See the Supporting Information for discussions on the shape of the curve.) Reported values for static characteristics are mean ± S.D. (n = 7 different samples). (In addition, $L(\Delta P,\sigma) - L(0,\sigma)$ is the change in length of the VAMP, F is the force due to difference of pressure, and T is the total loading force.) E) The relationship between force and velocity for VAMPs fabricated in Elastosil. F) The relationship between power density and stress for VAMPs fabricated in Elastosil. Reported values for dynamic characteristics are mean ± S.D. (n = 3 measurements).

high differential pressure ($\Delta P > \Delta P_{crit}$), increasing the loading stress σ decreases the actuation strain $s(\Delta P, \sigma)$ of VAMPs, and the maximum loading stress is reached when the actuation strain is close to 0. The maximum loading stress of VAMPs scales linearly with the Young's modulus of the actuator (see the Supporting Information for a theoretical validation; also see the Supporting Information for an explanation for the initial increase of actuation strain at low stress). A VAMP made of an elastomer with critical Young's Modulus ($E \approx 5$ MPa) has a projected loading stress of about 60 kPa at 30% actuation strain, and a loading stress of about 100 kPa at 0% actuation strain. Figure S2 and Movie S3 (Supporting Information) show a VAMP that demonstrates ≈65 kPa loading stress at 10% actuation strain when fabricated in a urethane elastomer with Young's modulus $E \approx 2.5$ MPa.

VAMPs made of materials with E > 5 MPa will not actuate fully under atmospheric pressure, but if P_{ext} is greater (e.g., in hyperbaric environments such as undersea), much greater forces could be generated, using stiffer elastomers, and an actuation cycle that includes positive pressure to inflate the VAMP to $\Delta P = 0$. The Supporting Information compares the force generated by VAMPs to biological muscle and other actuators.

We obtained the energy density of VAMPs fabricated in Elastosil (Figure S11, Supporting Information) by using the data from the force versus length plot of VAMPs (Figure 2D). For the VAMPs fabricated in Elastosil, the energy density peaks at ≈2 J L^{-1} or ≈3.7 J kg^{-1} (the density of VAMPs made of Elastosil is ≈0.54 kg L^{-1}, while the density of Elastosil itself is ≈1 kg L^{-1}). VAMPs made of materials with critical Young's modulus are projected to demonstrate a peak work output per unit volume of ≈20 J L^{-1}.

We characterized the dynamic characteristics of VAMPs (fabricated in Elastosil, with dimension 34 mm × 28 mm × 46.5 mm) by measuring their force–velocity relationships and power densities (the Supporting Information describes the method).

Figure 2E shows a force versus velocity curve (derived from the raw displacement, velocity, and acceleration data shown in Figure S10 (Supporting Information)). The VAMPs demonstrate a faster actuation speed with a lighter load. We note that neither the force nor the velocity in this plot represent the theoretical maximum. Here, the force can be enhanced ten times by using an elastic material that is capable of large deformation and has ten times the Young's modulus of Elastosil, while the velocity can be enhanced by using pneumatic input with a larger radius.

Figure 2F shows the power density of VAMPs as a function of velocity (derived from the force vs. velocity data in Figure 2E). For VAMPs fabricated in Elastosil, the power density peaks at ≈10 W L^{-1} (or ≈18.5 W kg^{-1}). VAMPs that are made of materials with critical Young's modulus, but maintain the same velocity, are projected to demonstrate a peak power output per unit volume of ≈100 W L^{-1}. The maximum power during isotonic contraction for natural skeletal muscles ranges from 7 to 500 W kg^{-1}.[37] As discussed previously, the velocity of these VAMPs is not at the physical limit. The Supporting Information compares the dynamic characteristics of VAMPs to those of biological muscle, and other various linear actuators. We also include in the Supporting Information a modeling approach to better analyze the dynamic characteristics of VAMPs (also see Figure S8, Supporting Information).

When vacuum is applied to their internal chambers, the principle contraction of VAMPs is uniaxial (with little change of cross-sectional area), in a direction determined by the pattern of their internal soft structures (Figure 1). These patterns can extend over substantial lengths and areas. Increasing the length increases the total displacement of the VAMPs on actuation, and increasing the cross-sectional area increases the force they generate (for example, in **Figure 3** and Movies S4 and S5 (Supporting Information)). In Figure 3A, the length of the

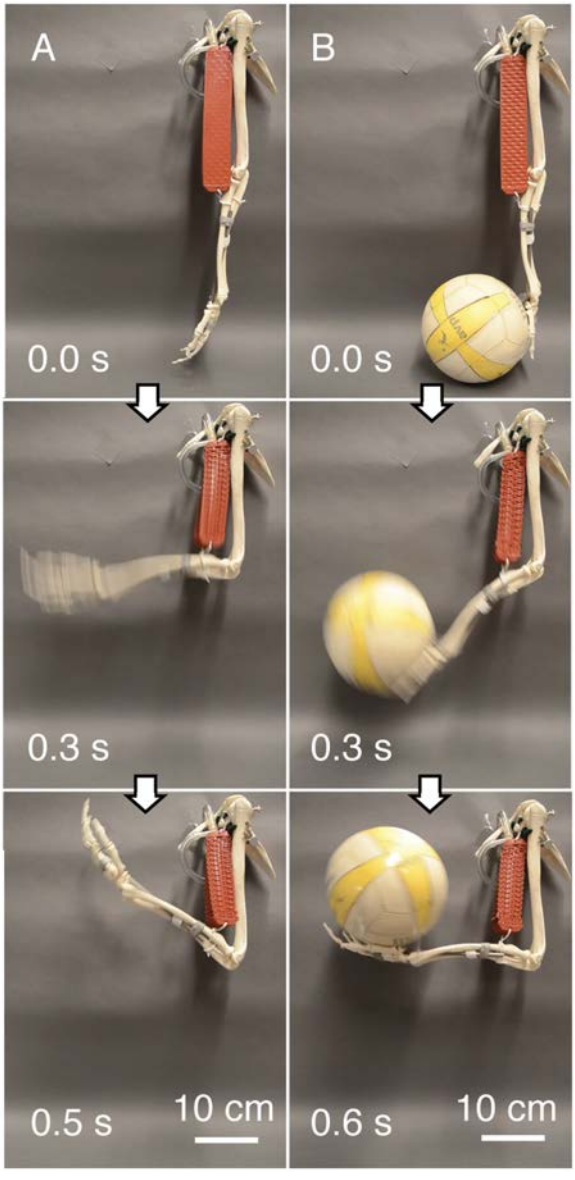

Figure 3. Demonstration of muscle-like actuation. A) Use of a VAMP to actuate a polymer replica of the bones of a human arm, with mechanics similar to that employed by a human bicep muscle. Here metal wires serve as "tendons" to connect VAMP and replica bone, but high tensile strength polymer fibers could serve equally well. B) The VAMP-actuated "arm" lifting a volleyball of standard size and weight (274 g). See Movies S4 and S5 (Supporting Information) for the videos. (See Figure S5 and Movies S6 and S7 (Supporting Information) for speed comparison with a fast-moving human arm.)

VAMP decreased by ≈30% on actuation; the resulting displacement of the "hand" was about five times the change in length of the VAMP, because the lever arm ratio was 1:5 (a value similar to that of a human arm[38]). We also show that the speed of this "arm-like" structure driven by a VAMP is comparable to a human arm (see Figure S5 and Movies S6 and S7 (Supporting Information)).

The relatively high speed of VAMPs allows them to perform tasks that are more dynamic than simple lifting (even without a complex control system). Figure S12 (Supporting Information) shows that the "arm-like" structure can flip a cup in the palm of its "hand" into an upright position by using a jerking motion, which would not be possible with a slow muscle (see Movie S8, Supporting Information). Figure S13 (Supporting Information) shows more demonstrations of the "arm-like" structure actuated by a VAMP in performing other muscle-like tasks (Movies S9 and S10, Supporting Information). Humans and animals can perform more complex motions or sequences of motions by mobilizing a collection of many muscles and coordinating them with a neural network. By incorporating a collection of VAMPs of different sizes and coordinating them with an appropriate control system (not demonstrated in this work), biomimetic machines might imitate motions of more complex animal structures.

Being soft and actuated by vacuum, VAMPs possess many intrinsic functional traits that are not present in hard linear actuators, or in pressure-actuated structures (e.g., McKibben actuators). Examples include functional traits such as compliance, shock absorbance, nondamaging interaction with the environment, and elastic energy storage (see Figure S7 (Supporting Information)). Vacuum actuation allows VAMPs to be installed in space-limited positions (such as inside a rigid pipe). VAMPs also preserve their function and performance even after punctures. For example, the actuation was unchanged after a VAMP was punctured with a 2 mm-wide metal cannula (Figure S6 and Movie S11, Supporting Information). We attribute this self-sealing ability of VAMPs to compression around the puncture by atmospheric pressure and elastomeric retraction.

The thermodynamic efficiency of transduction of the pressure–volume work required to actuate VAMPs into mechanical (force × distance) work (e.g., lifting a weight) is limited by the work required to compress the elastomer. By comparison, the loss of energy due to hysteresis is small (details are in Figure S3 (Supporting Information)). Our experimental data gave a thermodynamic efficiency of 27% for an actuation strain of 20% at 500 g loading for the VAMP shown in Figure 1D (details of the method are in the Supporting Information). For comparison, the corresponding value of a human skeletal muscle is ≈40%.[27] The energy stored in the deformed, elastomeric components (which is not converted into useful mechanical work and thus reduces the thermodynamic efficiency for a single, unidirectional motion) can, in principle, be at least partially recovered during unloading. A system containing VAMPs can, therefore, have a greater efficiency over multiple actuation cycles than that measured in a single cycle. (This method of storing and recovering energy of soft actuators has been reported in a number of designs.[27])

The mechanism by which VAMPs achieved their mechanical performance demonstrates a new approach for biomimetic actuation: nonlinear motion reflecting the cooperative, reversible, buckling, and collapse of elastomeric beams. VAMPs have eight characteristics that will be useful in soft machines: (i) no expansion in volume on contraction; (ii) many aspects of mechanical performance on actuation similar to human muscle; (iii) they are "collaborative" (to use the term common in robotics)—that is, safe in use around humans; (iv) thermodynamic efficiency comparable to (although currently less than) muscle; (v) a cost of fabrication sufficiently low that they can be considered for single-use applications; (vi) performance that is reliable even after a high number of actuation cycles (VAMPs fabricated in Elastosil demonstrated no significant change in performance after a million cycles of actuation; Figure S4 (Supporting Information)); (vii) light weight and low density (relative to metals); (viii) properties characteristic of organic polymers (transparency, electrical properties that extend from insulating to conducting, biocompatibility, controllable rates of environmental degradation, ease of fabrication in complex shapes) that will be useful in specific applications.

VAMPs are not (and not intended to be) competing with hard actuators. They are complimentary, and intended largely for noncompetitive and hybrid uses: examples would include assistive devices for the elderly or disabled, systems for non-damaging manipulation of irregularly shaped and delicate objects (fruit, tissues, small animals), devices intended to be inexpensive enough for single use (e.g., in search and rescue), or where resistance to damage by impact are important, and others where soft systems offer capabilities not easily or inexpensively embedded in hard systems with typical designs.

The designs of the actuators used in Figures 1 and 3 are a small subset of those that can be created through appropriate design and segmentation of the patterns of pillars making up the VAMPs, and through extension of these quasi-2D structures into 3D. The key feature of all of these designs is, however, the use of cooperative, reversible buckling in an elastomeric material to achieve actuation. This work thus exploits buckling to achieve useful and simple (quasilinear) motion through a mechanism that involves complex, nonlinear, cooperative motions of the internal structure of the VAMPs.

Supporting Information

Supporting Information is available from the Wiley Online Library or from the author.

Acknowledgements

Work on biomimetic design was funded by a subcontract from Northwestern University under DOE award number DE-SC0000989. Work on thermodynamics and mechanics was funded by the DOE, Division of Materials Sciences and Engineering, grant number ER45852. M.S.V. was funded by the Banting Postdoctoral Fellowship from the Government of Canada. B.M. and C.K. acknowledge the Wyss Institute for Biologically Inspired Engineering for partial salary support. B.L. was supported by a Harvard University work-study program for undergraduates. F.K. was supported by the NSF-funded REU program under award number DMR-0820484.

Received: April 1, 2016
Revised: April 24, 2016
Published online: June 1, 2016

[1] D. Rus, M. T. Tolley, *Nature* **2015**, *521*, 467.
[2] B. Trimmer, *Curr. Biol.* **2013**, *23*, R639.
[3] S. Kim, C. Laschi, B. Trimmer, *Trends Biotechnol.* **2013**, *31*, 287.
[4] K. Suzumori, S. Iikura, H. Tanaka, *Proc. IEEE Int. Conf. Rob. Autom.* **1991**, 1622.
[5] E. Brown, N. Rodenberg, J. Amend, A. Mozeika, E. Steltz, M. R. Zakin, H. Lipson, H. M. Jaeger, *Proc. Natl. Acad. Sci. USA* **2010**, *107*, 18809.
[6] F. Ilievski, A. D. Mazzeo, R. F. Shepherd, X. Chen, G. M. Whitesides, *Angew. Chem., Int. Ed.* **2011**, *123*, 1930.
[7] R. V. Martinez, J. L. Branch, C. R. Fish, L. Jin, R. F. Shepherd, R. Nunes, Z. Suo, G. M. Whitesides, *Adv. Mater.* **2013**, *25*, 205.
[8] B. Mosadegh, P. Polygerinos, C. Keplinger, S. Wennstedt, R. F. Shepherd, U. Gupta, J. Shim, K. Bertoldi, C. J. Walsh, G. M. Whitesides, *Adv. Funct. Mater.* **2014**, *24*, 2163.
[9] C. C. De Wit, G. Bastin, B. Siciliano, *Theory of Robot Control*, Springer-Verlag, New York, NY, USA **1996**.
[10] M. W. Spong, S. Hutchinson, M. Vidyasagar, *Robot Modeling and Control*, Vol. *3*, Wiley, New York, NY, USA **2006**.
[11] C. C. Kemp, A. Edsinger, E. Torres-Jara, *IEEE Robotics Automat. Mag.* **2007**, *14*, 20.
[12] R. Bruzek, L. Biess, L. Al-Nazer, *Proc. ASME Jt. Rail Conf.* **2013**, V001T01A007.
[13] J. Gordo, C. Guedes Soares, D. Faulkner, *J. Ship Res.* **1996**, *40*, 60.
[14] J. Miller, T. Su, J. Pabon, N. Wicks, K. Bertoldi, P. Reis, *Int. J. Solids Struct.* **2015**, *72*, 153.
[15] S. Singamaneni, V. V. Tsukruk, *Soft Matter* **2010**, *6*, 5681.
[16] D. Chen, J. Yoon, D. Chandra, A. J. Crosby, R. C. Hayward, *J. Polym. Sci., Part B: Polym. Phys.* **2014**, *52*, 1441.
[17] N. Hu, R. Burgueño, *Smart Mater. Struct.* **2015**, *24*, 063001.
[18] J. A. Rogers, T. Someya, Y. Huang, *Science* **2010**, *327*, 1603.
[19] Y. Wang, R. Yang, Z. Shi, L. Zhang, D. Shi, E. Wang, G. Zhang, *ACS Nano* **2011**, *5*, 3645.
[20] J. Shim, C. Perdigou, E. R. Chen, K. Bertoldi, P. M. Reis, *Proc. Natl. Acad. Sci. USA* **2012**, *109*, 5978.
[21] B. Florijn, C. Coulais, M. Van Hecke, *Phys. Rev. Lett.* **2014**, *113*, 175503.
[22] P. Wang, F. Casadei, S. Shan, J. C. Weaver, K. Bertoldi, *Phys. Rev. Lett.* **2014**, *113*, 014301.
[23] A. Rafsanjani, A. Akbarzadeh, D. Pasini, *Adv. Mater.* **2015**, *27*, 5931.
[24] J. T. Overvelde, T. Kloek, J. J. D'haen, K. Bertoldi, *Proc. Natl. Acad. Sci. USA* **2015**, *112*, 10863.
[25] D. Yang, B. Mosadegh, A. Ainla, B. Lee, F. Khashai, Z. Suo, K. Bertoldi, G. M. Whitesides, *Adv. Mater.* **2015**, *27*, 6323.
[26] S. Timoshenko, J. M. Gere, *Theory of Elasticity Stability*, McGraw-Hill, New York, NY, USA **1961**.
[27] J. D. Madden, N. A. Vandesteeg, P. A. Anquetil, P. G. Madden, A. Takshi, R. Z. Pytel, S. R. Lafontaine, P. A. Wieringa, I. W. Hunter, *IEEE J. Oceanic Eng.* **2004**, *29*, 706.
[28] F. Daerden, D. Lefeber, *Eur. J. Mech. Environ. Eng.* **2002**, *47*, 11.
[29] G. K. Klute, J. M. Czerniecki, B. Hannaford, *Proc. IEEE Int. Conf. Adv. Intell. Mechatron.* **1999**, 221.
[30] C.-P. Chou, B. Hannaford, *IEEE Trans. Robot. Autom.* **1996**, *12*, 90.
[31] R. H. Baughman, *Science* **2005**, *308*, 63.
[32] G. Kovacs, L. Düring, S. Michel, G. Terrasi, *Sens. Actuators, A* **2009**, *155*, 299.
[33] Q. Pei, M. A. Rosenthal, R. Pelrine, S. Stanford, R. D. Kornbluh, *Smart Struct. Mater.* **2003**, 281.
[34] T. Mullin, S. Deschanel, K. Bertoldi, M. Boyce, *Phys. Rev. Lett.* **2007**, *99*, 084301.
[35] K. Bertoldi, M. Boyce, S. Deschanel, S. Prange, T. Mullin, *J. Mech. Phys. Solids* **2008**, *56*, 2642.
[36] M. Bowick, A. Cacciuto, G. Thorleifsson, A. Travesset, *Phys. Rev. Lett.* **2001**, *87*, 148103.
[37] R. Josephson, *Annu. Rev. Physiol.* **1993**, *55*, 527.
[38] M. Ikai, T. Fukunaga, *Int. Z. Angew. Physiol.* **1970**, *28*, 173.